Indian Journal of Chemical Technology
Vol. 17, November 2010, pp. 425-430

Inhibition of mild steel corrosion in 1 M hydrochloric acid using (E)-4-(2-chlorobenzylideneamino)-6-methyl-3-thioxo-3,4-dihydro-1,2,4-triazin-5(2H)-one (CBMTDT)

Bincy Joseph, Sam John, K K Aravindakshan & Abraham Joseph*
Department of Chemistry, University of Calicut, Calicut 673 635, India
*Email: drabrahamj@gmail.com

Received 1 December 2009; revised 28 July 2010

The use of nitrogen and sulphur donor organic inhibitors in acid solutions is a common method for the protection of metals from corrosion. The present work is the study of the corrosion inhibition efficiency of (E)-4-(2-chlorobenzylideneamino)-6-methyl-3-thioxo-3,4-dihydro-1,2,4-triazin-5(2H)-one (CBMTDT) towards mild steel in 1 M HCl. The work strategy includes the conventional weight loss method, potentiodynamic polarization studies (Tafel), linear polarization studies (LPR), electrochemical impedance spectroscopy (EIS), adsorption studies and quantum chemical calculations. Results showed that the corrosion rate decreases and inhibition efficiency increases with inhibitor concentration. The results of polarization studies reveal that the additive acts as a mixed type inhibitor. The surface adsorption of the inhibitor molecules decreases the double layer capacitance and increases the polarization resistance. The adsorption process is spontaneous and follows Langmuir adsorption isotherm model. The optimized structure of the inhibitor, energies of LUMO, HOMO and other physical parameters are calculated by computational quantum chemical methods.

Keywords: Corrosion, Mild steel, Electrochemical impedence, Potentiodynamic polarization, CBMTDT

The use of acid solution during pickling and industrial cleaning leads to corrosive attack on carbon steel. One of the most popular methods for the protection of metals in acidic solutions is the use of corrosion inhibitors[1-4]. Different groups of organic compounds have been reported to exert inhibitive effects on the corrosion of carbon steel. Molecules containing electronegative functional groups and pi electrons in triple or conjugated double bonds are particularly effective. It has been reported that nitrogen containing inhibitors are useful in hydrochloric acid solution, while sulphur containing inhibitors exert excellent efficiencies in sulphuric acid[5,6]. These inhibitors can adsorb on the metal surface through the heteroatom such as nitrogen, oxygen and sulphur and block the active sites and decrease the corrosion rate[7-10]. The aim of the present work is to investigate the corrosion inhibition efficiency of (E)-4-(2-chlorobenzylideneamino)-6-methyl-3-thioxo-3,4-dihydro-1,2,4-triazin-5(2H)-one (CBMTDT) towards mild steel in 1 M HCl using gravimetric and electro analytical techniques.

Experimental Procedure

Preparation of inhibitor

The inhibitor, CBMTDT (Fig. 1) was prepared by condensing 4-amino-3-mercapto-6-methyl-1, 2, 4-triazin-4H-one with o-chlorobenzaldehyde. The former compound was synthesized in the laboratory by reacting pyruvic acid with thiocarbohydrazide (E. Merck). The recrystallised sample was characterized by various physico-chemical methods. The compound is soluble in 1 M HCl at room temperature.

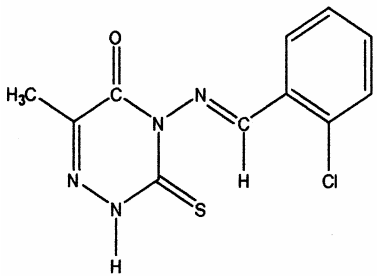

Fig. 1—Structure of the inhibitor molecule

Medium

The medium for the study was prepared from reagent grade HCl (E. Merck) and doubly distilled water. The entire tests were performed in aerated medium under standard conditions.

Materials

The steel sample had the following composition: C, 0.2; Mn, 1; P, 0.03; S, 0.02; and Fe, 98.75%. The mild

steel specimens used in weight loss measurements were cut in 4.8×1.9×0.12 cm^3 coupons. For electrochemical studies, same types of coupons were used but only 1 cm^2 area was exposed in each tests. Before both the measurements the samples were polished using different grades of emery papers, degreased by washing with ethanol, acetone and finally washed with distilled water.

Weight loss measurements

The weight loss experiments were carried out under total immersion conditions in test solution maintained at room temperature. For weight loss studies the required number of specimens of above-mentioned size were cut and cleaned in acid solutions for removing rust particles and later polished with 1-4/0 finer grades of emery paper to mirror bright finish. All specimens were cleaned according to ASTM standard G-1-72 procedure[11-16]. The experiments were carried out in a beaker containing 250 mL solution. After exposure, the specimens were removed, washed initially under running tap water, to remove the loosely adhering corrosion product and finally cleaned with a mixture of 20% NaOH and 200 g/L zinc dust followed by acetone. Then the loss in weight was determined by analytical balance having a sensitivity of 0.1 mg. Similar experiments were conducted with different inhibitor concentrations to find out the effect of inhibitor concentration towards corrosion rate and inhibition efficiency. In each case duplicate experiments were conducted. The second results were within $\pm$1% of the first. Whenever the variations were very large, the data were confirmed by a third test. The percentage inhibition efficiency, % IE was calculated using the relation:

$$\% \text{ IE} = \frac{W_0 - W}{W_0} \times 100 \quad \ldots (1)$$

where W_0 and W are the weight losses in the uninhibited and inhibited solutions respectively.

Electrochemical measurements

Electrochemical test were carried out in a conventional three-electrode configuration with platinum sheet (surface area, 1 cm^2) as auxiliary electrode and saturated calomel electrode (SCE) as the reference electrode. The working electrode was first immersed in the test solution and after establishing a steady state OCP the electrochemical measurements were carried out with a Gill A C computer controlled electrochemical workstation (ACM, U.K model no: 1475). The potentiodynamic polarization curves were obtained in the potential range from –250 to +250 mV with a sweep rate of 1000 mV/min (16 mV/s) and electrochemical impedance spectroscopy (EIS) measurements were carried out with amplitude of 10 mV ac sine wave with a frequency range of 10 KHz to 10 Hz with reference to standard calomel electrode (SCE).

Quantum chemical calculation

Quantum chemical calculation were performed based on ab initio method and 6-31G* basis set. The basis set provide information about mullicken charges, energies of highest occupied molecular orbital (HOMO), lowest unoccupied molecular orbital (LUMO) etc.

The chemical reactivity of different sites of the molecules was evaluated by Fukui indices, as defined by:

For nucleophilic attack

$$\int_k^+ = q_{N+1} - q_N$$

For electrophilic attack

$$\int_k^- = q_N - q_{N-1}$$

where q_N, q_{N-1} and q_{N+1} are the electronic population of the atom k in neutral, cationic and anionic systems, respectively[17,18]. The condensed Fukui function is local reactivity descriptor and can be used only for comparing reactive atomic centers within the same molecule. Condensed softness indices allow the comparison of reactivity between similar atoms of different molecules starting from the relation between the Fukui function $\int(r)$ and the local softness S(r).

$$S(r) = (\partial\rho(r)/\partial N)_{v(r)}(\partial N/\partial\mu)_{v(r)} = \int(r)S$$

All calculations, including geometry optimization of the inhibitor were performed with the B3LYP exchange correlation corrected functional with the 6-31G (d) basis set using the Gaussian 03W package. As shown by De Proft *et al.*[21], the B3LYP functional appears to be reliable for calculating $\int$ (r) and $\int_k$ indices.

Results and Discussion

Weight loss studies

From these studies it is clear that the weight loss enhances with increasing exposure time and decreases

with increasing inhibitor concentration. The weight loss data were used to calculate the corrosion rate using the equation:

$$\text{Corrosion rate} = \frac{534W}{DAT}$$

where W is the loss of weight (mg), D is the density of the specimen, A is the area of the specimen and T is the exposure time in hours. The results of the variations of corrosion rate with exposure time are given in Table 1. The corrosion rate decreases with increasing concentration of CBMTDT.

Potentiodynamic polarization studies

Potentiodynamic polarization studies of mild steel in 1 M HCl in the absence and presence of inhibitors were also carried out. The cathodic and anodic polarization curves obtained with various inhibitor concentrations are shown in Fig. 2. The electrochemical parameters like corrosion potential (E_{corr}), cathodic and anodic Tafel slopes (β_c and β_a) and corrosion current density (i_{corr}) obtained from Tafel extrapolation of polarization curve are given in Table 2. The corrosion inhibition efficiency was calculated using the relation:

$$\%\text{IE} = \frac{i_{corr^*} - i_{corr}}{i_{corr^*}} \times 100 \quad \ldots (2)$$

where i_{corr}* and i_{corr} are uninhibited and inhibited corrosion current densities, respectively. It is clear from the figure that both the anodic metal dissolution and cathodic hydrogen evolution reactions were inhibited after the addition of CBMTDT to the aggressive medium. The change in the slope of cathodic current-potential line and anodic current-potential line indicates the modification of both anodic and cathodic reaction mechanisms in inhibited solution with time. These results suggest that CBMTDT acts as mixed type corrosion inhibitor[22]. The inhibitor molecules are first adsorbed onto the metal surface and impede by merely blocking the metal sites without affecting the anodic and cathodic reaction mechanism[23]. The corrosion current density decreased and inhibition efficiency increased with increasing inhibitor concentration which may be due to the increase of surface coverage. Linear polarization resistance plot (LPR) is another form of Tafel plot and is depicted in Fig. 3. Polarization resistance (R_p) was determined from the slope of the potential versus current lines (LPR plot) and is presented in Table 2. The increase of R_p values with increasing inhibitor concentration is due to the adsorption of inhibitor molecule on the metal surface.

Table 1—Corrosion rate of mild steel in 1 M HCl solution in the presence of various concentrations of CBMTDT

Conc. (ppm)	Corrosion rate (mpy) with time in hours			
	24	48	72	96
0	12875	8881	6148	4741
10	11537	7111	4927	3874
25	1724	1090	892	743
50	1559	972	710	606
75	1445	870	674	542
100	952	751	582	478
200	851	621	473	387

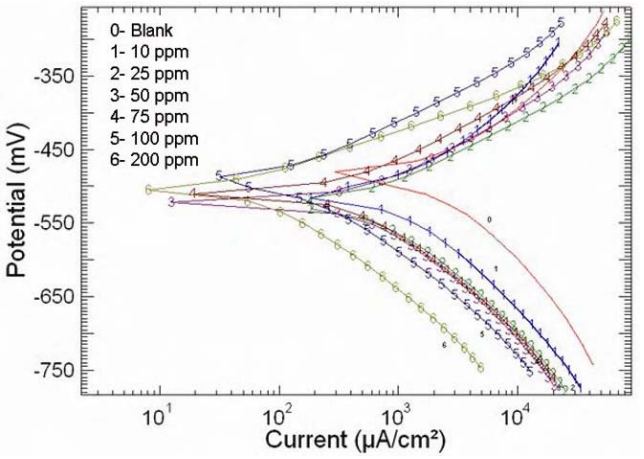

Fig. 2—Potentiodynamic polarization curve for MS in 1 M HCl in the absence and presence of different concentration of CBMTDT at 300 K

Table 2—Electrochemical parameters for mild steel obtained from polarisation curves in 1 M HCl at 300 K.

Conc. (ppm)	E_{corr} (mV)	R_p (Ω cm^2)	β_a (mV dec^{-1})	β_c (mV dec^{-1})	i_{corr} (μA cm^{-2})	% IE	C.R. (mpy)	Surface coverage (Θ)
0	-484	8	21	144	3601	—	601	—
10	-501	11	101	139	1841	50	360	0.4009
25	-515	13	75	102	1622	55	239	0.6023
50	-509	16	80	121	1443	61	140	0.7670
75	-510	19	109	167	1304	63	99	0.8352
100	-500	40	66	113	443	87	27	0.9550
200	-504	35	67	66	412	89	13	0.9783

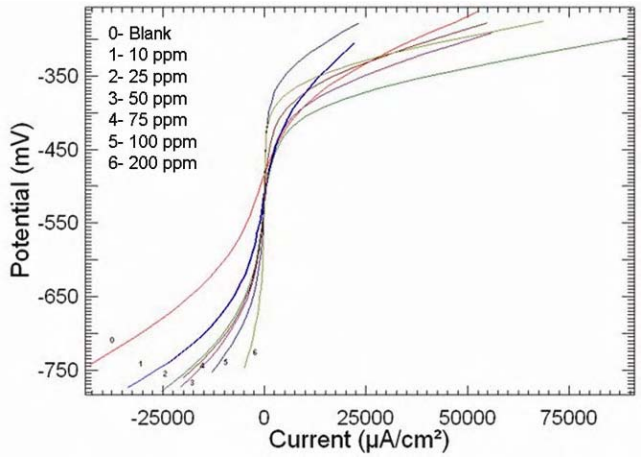

Fig. 3—Linear polarization curves for MS in 1 M HCl in the absence and presence of different concentrations of CBMTDT at 300 K

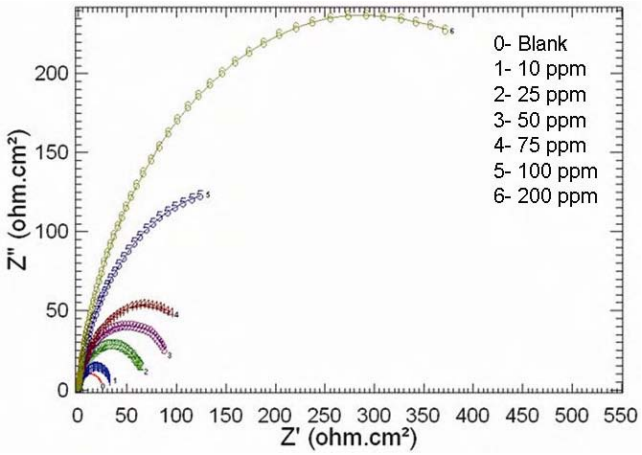

Fig. 4—Nyquist plots for MS in 1 M HCl in the absence and presence of different concentrations of CBMTDT at 300 K

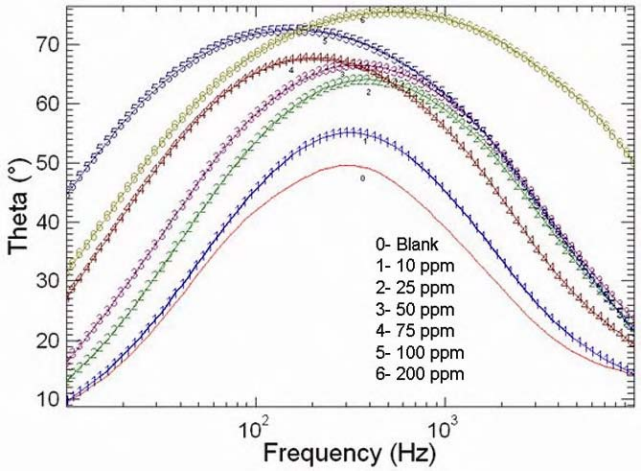

Fig. 5—Bode curves for MS in 1 M HCl in the presence of different concentrations of CBMTDT at 300 K

Thus LPR also agrees with the above-discussed adsorption mechanism of the inhibition.

Electrochemical impedance spectroscopy

EIS technique provides a rapid and convenient method to evaluate the performance of the organic coating on the metals and has been used for the investigation of protective nature of organic inhibitors. The inhibitor does not disturb the double layer at the metal/solution interface. Therefore, results that are more reliable can be obtained from this technique. The Nyquist plot and the representative Bode diagrams for the mild steel after 1 h exposure in uninhibited and inhibited 1 M HCl are dipicted in Figs 4 and 5. The semicircular appearance of the impedance diagram indicates that the corrosion of mild steel is controlled by a charge transfer process[24]. Polarization resistance which corresponds to the diameter of Nyquist plot includes charge transfer resistance (R_{ct}), diffuse layer resistance (R_d), accumulation resistance (R_a), film resistance (R_f), etc. The charge transfer resistance determines the corrosion rate corresponding to the resistance between the metal and Outer Helmholtz Plane (OHP)[25,26]. Table 3 lists the important parameters obtained from impedance spectra. R_{ct} and C_{dl} values have opposite trend throughout the analysis. The decrease in electrical double layer capacitance with increase in inhibitor concentration may be attributed to the formation of a protective layer on the electrode surface which may be responsible for reducing the corrosion rate. The adsorbed layer of the inhibitor molecule displaces the water molecule and other ions originally adsorbed on the metal surface[27]. The values of corrosion inhibition efficiency (%IE) are calculated using the Eq. (3) and are included in Table 3.

$$\%\text{IE} = \frac{R_{ct^*} - R_{ct}}{R_{ct^*}} \times 100 \quad \ldots (3)$$

Table 3—AC impedance data of mild steel with CBMTDT at 300 K in 1 M HCl

Conc. (ppm)	R_{ct} (Ω cm^2)	C_{dl} (μF cm^{-2})	i_{corr} (μA cm^{-2})	%IE	C.R. (mpy)
0	23	220	1120	----	512
10	31	130	817	27	373
25	69	111	377	66	172
50	100	102	259	77	118
75	132	106	197	82	90
100	300	99	86	92	39
200	579	31	45	96	20

where R_{ct*} and R_{ct} are values of the charge transfer resistance observed in the presence and absence of CBMTDT. The results obtained from the electrochemical measurements support the data derived from weight loss measurements.

Adsorption studies

The adsorption isotherm can provide basic information on the interaction of inhibitor with metal surface[28,29]. To obtain adsorption isotherm, the surface coverage values (θ) for different concentrations of inhibitor in 1 M HCl have been obtained from potentiodynamic polarization measurements. Using these data different graphs has been constructed to find out the most suitable adsorption isotherm. The plot Log (θ/1-θ) versus Log C yields a straight line with a slope of 1.4416 and R^2=0.9139, indicating that the adsorption of the CBMTDT on mild steel surface obeys Langmuir adsorption isotherm (Fig. 6).

Quantum chemical calculations

To study the effect of molecular structure on the inhibition efficiency of the CBMTDT, *ab initio* quantum chemical calculations were performed using density functional theory (DFT). The mullikken charge distribution on the inhibitor molecule ranges from -0.616 to 0.616. The quantum chemical values were computed using DFT and energies of highest occupied molecular orbital (E_{HOMO} = -1.8231eV), lowest unoccupied molecular orbital (E_{LUMO} = -5.7555 eV) and total energy (E_{total} = 795676.40 kcal/mol) are calculated. The dipole moment of the molecule is calculated to be 4.0852D. It has been observed that the inhibition efficiency of a molecule is related to the inhibitor-metal orbital interactions. Good inhibitor molecules offer electrons to the unoccupied orbital of metal and accept free electrons from the metal. That is a charge transfer phenomenon may takes place between the metal and the inhibitor molecules, which confirms that adsorption of the inhibitor is the basis for inhibitory action towards mild steel in 1 M HCl. From quantum chemical calculations, it is clear that higher the HOMO energy of the inhibitor, greater is the trend of donating electrons to the unoccupied 'd 'orbital of the metal, and higher the corrosion inhibition efficiency. The lower LUMO energy level makes easy acceptance of electrons from the metal surface. The magnitude of ΔE value, ($\Delta E = E_{LUMO} - E_{HOMO}$) also helps to predict probable routs of the inhibitory action[30,31]. Smaller the ΔE value greater is the inhibitory action. Here the lower value of ΔE also agrees with the excellent inhibition efficiency of CBMTDT towards mild steel in 1 M HCl solution.

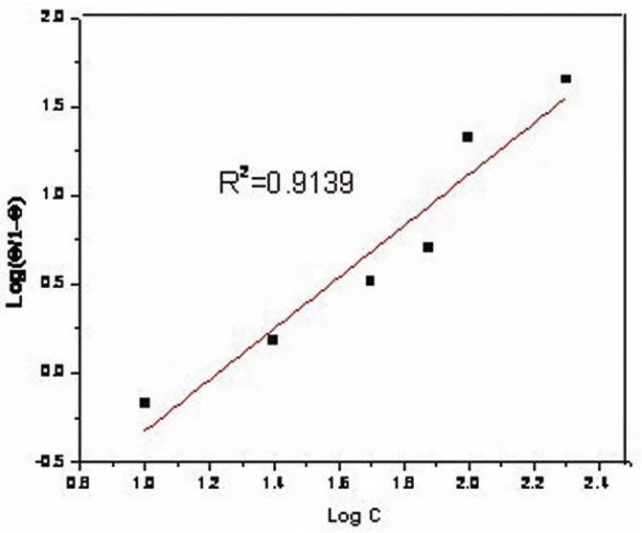

Fig. 6— Langmuir adsorption isotherm for MS in 1 M HCl at 300 K in the presence of CBMTDT

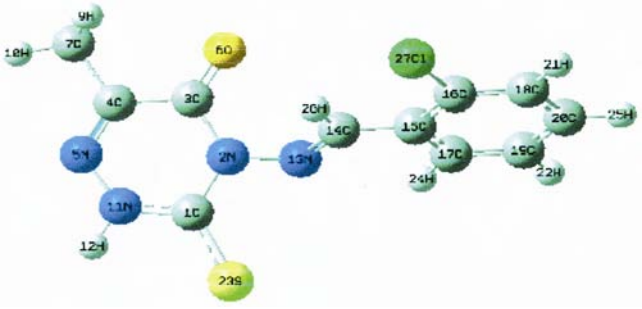

Fig. 7—Optimized geometry of the CBMTDT molecule

Local selectivity

The local reactivity of CBMTDT is analyzed by means of the condensed Fukui function. The condensed Fukui functions and condensed local softness indices allow one to distinguish each part of the molecule on the basis of its distinct chemical behaviour due to the different substituent functional groups[32]. Thus, the site for nucleophilic attack will be the place where the value of $\int^+$ is the maximum. In turn, the sight for electrophilic attack is controlled by the value of $\int^-$. For nucleophilic attack the most reactive site of CBMTDT is on the C (14) atom. For electrophilic attack the most reactive site of CBMTDT is on the S (23) atom. It is clear that C (14) has more nucleophilic character and is involved in the chemical reactivity of the molecule with metal surface, which explains the adsorption mechanism of inhibitor on mild steel surface in hydrochloric acid. The optimized geometry of CBMTDT is given in Fig. 7 and the results are given in Table 4. The condensed local softness indices Sk^- and Sk^+ are related to the condensed Fukui

Table 4—Fukui functions and local softness values for CBMTDT

	Atom	f(-)	f(+)	Sk(+)	Sk(-)
1	C	0.0438	0.0330	0.1022	0.0770
2	N	0.0110	0.0244	0.0257	0.0569
3	C	0.0023	0.0580	0.0054	0.1354
4	C	0.0007	0.0813	0.0016	0.1897
5	N	0.0123	0.1001	0.0287	0.2336
6	O	0.0066	0.0398	0.0541	0.0929
7	C	0.0008	0.0011	0.0019	0.0026
8	H	0.0001	0.0024	0.0002	0.0056
9	H	0.0002	0.0025	0.0005	0.0058
10	H	0.0001	0.0000	0.0002	0.0000
11	N	0.0101	0.0082	0.0236	0.0191
12	H	0.0056	0.0001	0.0131	0.0002
13	N	0.0215	0.1243	0.0502	0.2901
14	C	0.0069	0.1697	0.0161	0.3961
15	C	0.0021	0.0532	0.0049	0.1242
16	C	0.0022	0.0580	0.0051	0.1354
17	C	0.0017	0.0701	0.0039	0.1636
18	C	0.0002	0.0114	0.0005	0.0266
19	C	0.0005	0.0081	0.0017	0.0189
20	C	0.0032	0.1129	0.0075	0.2635
21	H	0.0000	0.0000	0.0000	0.0000
22	H	0.0000	0.0000	0.0000	0.0000
23	S	0.8656	0.0356	2.0204	0.0830
24	H	0.0000	0.0001	0.0000	0.0002
25	H	0.0000	0.0000	0.0000	0.0000
26	H	0.0015	0.0007	0.0035	0.0016
27	Cl	0.0010	0.0051	0.0023	0.0119

functions. The local softness follows the same trend of Fukui functions.

Conclusion

From the results of the study the following conclusions can be drawn:

(i) The compound, CBMTDT in 1 M HCl possesses excellent inhibition efficiency for mild steel corrosion.

(ii) As the concentration of the inhibitor increases, corrosion inhibition efficiency and charge transfer resistance increases whereas the corrosion rate and double layer capacitance decrease due to more adsorption of the inhibitor.

(iii) The inhibitor molecule affects both the anodic and cathodic processes and hence acts as a mixed type inhibitor.

(iv) The adsorption of the inhibitor obeys Langmuir adsorption isotherm model.

(v) Quantum chemical calculations show that, the increase in the energy of the HOMO of the inhibitor molecule promotes its tendency of electron donation to the unoccupied 'd' orbital of the metal and the lowering of the energy of the LUMO tend to increase its electron accepting power and the combined effect also increases the corrosion inhibition efficiency.

Acknowledgement

The authors are grateful to Kerala State Council for Science Technology and Environment (KSCSTE) for financial support in the form of a major research project 018/SRSPS/2006/CSTE.

References

1 Mihit M, El Issami S, Bouklah M, Bazzi L, Hammouti B, Ait Addi E, Salghi R & Kertit S, *Appl Surf Sci*, 252 (2006) 2389.
2 Mihit M, El Issami S, Bouklah M, Bazzi L, Hammouti B, Ait Addi E & Kertit S, *Pigm Resin Technol,* 35 (2006) 151.
3 Dafali A, Hammouti B, Mokhlisee & Kertit S, *Corros Sci,* 45 (2003) 1619.
4 Kertit S, Salghi R, Bazzi L, Hammouti B & Bouchtart A, *Ann Chim Sci Mater*, 25 (2000) 187.
5 Agrawal R & Namboodhiri T K G, *Corros Sci*, 39 (1990) 39.
6 Larabi L, Benali O & Harek Y, *Mater Lett*, 61 (2007) 3287.
7 Abdallah M, *Corros Sci,* 45 (2003) 2705.
8 Quraishi M A & Sardar R, *Mater Chem Phys,* 78 (2002) 425.
9 Sahin M, Bilgic S & Yilmaz H, *Appl Surf Sci,* 195 (2002) 1.
10 Yurt A & Balaban A, *Mater Chem Phys,* 85 (2004) 420.
11 Bag, S K, Chakraborty S B & Chaudhari S R, *J Indian Chem Soc*, 70 (1993) 24.
12 Ailor W H, *Hand book of corrosion testing and evaluation* (John Wiley and Sons, New York), 1971.
13 Talati J D & Modi R M, *Br Corros J,* 10 (1975) 103.
14 Talati J D & Patel G A, *Br Corros J,* 11 (1976) 47.
15 Champion F A, *Corrosion Testing Procedure*, 2nd edn (Chapman and Hall, London), 1964.
16 Fontana M G & Greene N D, *Corrosion Engineering* (McGraw Hill), 1984.
17 Parr R G & Yang W, *DFT of atoms and molecules* (Oxford University Press, Oxford), 1989.
18 Reed A E, Curtiss L A & Weinhold F, *Chem Rev,* 88 (1988) 899.
19 Becke A D, *J Chem Phys,* 98 (1993) 5648.
20 LeeYang W & Parr R G, *Phys Rev,* B37 (1988) 785.
21 Proft F de, Martin J M L & Geerlings P, *Chem Phys Lett,* 256 (1996) 400.
22 Fuchs-Godec R, *Colloids Surf A: Physicochem Eng Aspects,* 280 (2006) 130.
23 Abdel-Rehim S S, Ibrahim M A M & Khaled K F, *Mater Chem Phys,* 70 (2001) 268.
24 Hui-Long Wang, Rui-Bin Liu & Jian Xin, *Corros Sci,* 46 (2004) 2455.
25 Erbil M, *Chim Acta Turcica,* 1 (1988) 59.
26 Solmaz R, Kardas G, Yazici B & Erbil M, *Colloids Surf A,* 312 (2008).
27 Lebrini M, Lagrenee M, Vezin H, Gengembre L & Bentiss F, *Corros Sci,* 47 (2005) 485.
28 Migahed M A, Monhamed H M & Al-Sabagh, *Mater Chem Phys,* 80 (2003) 169.
29 Azim A, Shalaby L A & Abbas H, *Corros Sci,* 14 (1974) 21.
30 Lukovits I, Palfi K & Kalman E, *Corros Sci,* 53 (1997) 915.
31 Ozcan M & Dehri I, *Prog Org Coat,* 51 (2004) 181.
32 Fukui K, Yonezawa T & Shingu H, *J Chem Phys,* 20 (1952) 722.